



Deposited via The University of York.

White Rose Research Online URL for this paper:

<https://eprints.whiterose.ac.uk/id/eprint/170852/>

Version: Accepted Version

Article:

McLeish, Thomas Charles and Schaefer, Charley (2021) Power Law Stretching of Associating Polymers in Steady-State Extensional Flow. *Physical Review Letters*. 057801. ISSN: 1079-7114

<https://doi.org/10.1103/PhysRevLett.126.057801>

Reuse

This article is distributed under the terms of the Creative Commons Attribution (CC BY) licence. This licence allows you to distribute, remix, tweak, and build upon the work, even commercially, as long as you credit the authors for the original work. More information and the full terms of the licence here:

<https://creativecommons.org/licenses/>

Takedown

If you consider content in White Rose Research Online to be in breach of UK law, please notify us by emailing eprints@whiterose.ac.uk including the URL of the record and the reason for the withdrawal request.

Power-Law Stretching of Associating Polymers in Steady-State Extensional Flow

Charley Schaefer^{1,*} and Tom C. B. McLeish¹

¹*Department of Physics, University of York, Heslington, York, YO10 5DD, UK*

(Dated: January 4, 2021)

We present a tube model for the Brownian dynamics of associating polymers in extensional flow. In linear response, the model confirms the analytical predictions for the sticky diffusivity by Leibler-Rubinstein-Colby theory. Although a single-mode DEMG approximation accurately describes the transient stretching of the polymers above a ‘sticky’ Weissenberg number (product of the strain rate with the sticky-Rouse time), the pre-averaged model fails to capture a remarkable development of a power-law distribution of stretch in steady-state extensional flow: while the mean stretch is finite, the fluctuations in stretch may diverge. We present an analytical model that shows how strong stochastic forcing drives the long tail of the distribution, gives rise to rare events of reaching a threshold stretch, and constitutes a framework within which nucleation rates of flow-induced crystallization may be understood in systems of associating polymers under flow. The model also exemplifies a wide class of driven systems possessing strong, and scaling, fluctuations.

The natural or artificial production of high-performance polymeric materials requires precise control over flow-induced crystallization. This phenomenon involves in turn a highly non-trivial interdependence between the molecular level of bond-orientation-dependent nucleation, and the macroscopic level, where the temperature-dependent rheology generates stretch of entire chain segments [1–5]. Remarkably, nature has found a way to control robustly the flow-induced self-assembly of silk from an intrinsically disordered state (a solution of random-walk polymers) prior to forming high-performance fibers under flow at ambient conditions [6–14]. Key to achieving the final properties is that silk is processed in semi-dilute aqueous conditions [10], where nucleation can be induced through the stretch-induced disruption of the solvation layer [15]. How sufficient polymer stretch can be achieved in a limited time under modest flow conditions [9, 16] has so far remained unexplained. An important clue has been the observation of *strain hardening* [9, 16], which in *B. mori* silk [16] turned out to be triggered by a small number of calcium bridges [14, 17] that act as ‘sticky’ reversible intermolecular crosslinks akin to those in synthetic ‘sticky polymers’ [18–26]. For this class of molecules, a molecular understanding of the non-linear rheology and crystallization of sticky polymers has so far relied on computationally expensive (albeit coarse-grained to some degree) molecular dynamics simulations [5, 27–32]. Simpler molecular models coarse-grained at the level of entanglements, but able to capture the vital slow processes, remain absent.

In the present work, we address this need by following the central idea by de Gennes and Edwards of replacing the many-chain problem with a single chain in a tube-like confinement imposed by its environment of entanglements [33, 34], and solve the Brownian dynamics of the chain in 1D [35]. This approach is simple yet powerful, and has led to the development of widely applied finite-element solvers [36–39], a physical explana-

tion for the (apparent) 3.4 power dependence of the relaxation time of polymer melts on the molecular-weight [40], and a comprehensive understanding of the rich non-linear rheology of (bimodal) polymer blends [41, 42]. In the spirit of other theory and modeling work on associating polymers [38], in this letter we add a description for the stochastic attachment and detachment of associating monomers to the tubular environment developed for full non-linear flows. The model shares some structural similarities with early ‘transient network’ approaches to polymer melt and solution rheology [43], also demonstrating a hitherto unrecognised feature of those models.

The starting point of our contribution is to consider a chain consisting of N Kuhn segments with length b , and Z_e entanglements (hence, with tube diameter $a = b(N/Z_e)^{1/2}$). The configuration of the chain is given by the spatial coordinates R_i of monomers $i = 1, \dots, N$ along the curvilinear direction along the tube, which evolve with time according to the Langevin equation [35, 40, 41]

$$\zeta \frac{\partial R_i}{\partial t} = \left(\frac{3k_B T}{b^2} \frac{\partial^2 R_i}{\partial i^2} + f_i \right) (1 - p_i) + \dot{\epsilon} \zeta R_i, \quad (1)$$

with $\partial R/\partial i = a$ at $i = 1$ and at $i = N$, ζ the monomeric friction, $k_B T$ the thermal energy, and f_i a stochastic force given by the equipartition theorem

$$\langle f_i(t) \rangle = 0; \quad \langle f_i(t) f_{i'}(t') \rangle = 2k_B T \zeta \delta(i' - i) \delta(t' - t). \quad (2)$$

In the absence of stickers, this equation predicts the Rouse diffusivity [34]

$$D_R = \frac{a^2}{3\pi^2 \tau_e Z_e} = \frac{k_B T}{\zeta N} \quad (3)$$

and the variance of quiescent contour-length fluctuations $\langle |R_N - R_1|^2 \rangle = aZ_e/3$. The strain rate, $\dot{\epsilon}$, is in one spatial dimension equivalent to the strain rate in the GLaMM model [41].

73 To model the binding and unbinding of monomers to
 74 the environment, we introduce a stochastic state vari-
 75 able $p_i(t)$, which takes values of either zero or unity for
 76 each monomer i , which represents the ‘open’ and ‘closed’
 77 states of a monomer, respectively. An open monomer i
 78 is unbound and is free to diffuse and respond to the drag
 79 exerted by the flow field, as well as to relax stress in ad-
 80 joining segments. If this monomer represents a sticker,
 81 it may close through either association or bond-swapping
 82 events [44, 45]. The effective closing rate, $k_{i,\text{close}}$, sets the
 83 probability $1 - \exp(-k_{i,\text{close}}\Delta t) = k_{i,\text{close}}\Delta t + \mathcal{O}(\Delta t^2)$ of
 84 closing after a time interval Δt for small Δt . In every
 85 time step of our simulations a random number $r \in [0, 1]$
 86 is drawn and the sticker is closed if $r < k_{i,\text{close}}\Delta t \ll 1$
 87 [37] and is now kinetically trapped by its environment
 88 and is unable to diffuse or to respond to local stress in
 89 the polymer. Hence, the closed sticker advects with the
 90 background flow. The sticker may re-open according to
 91 the same recipe as above, but now with an opening rate
 92 $k_{i,\text{open}}$.

93 In principle, for copolymers or polymers with in-
 94 tramolecular (secondary) structures, each monomer can
 95 have different opening and closing rates. Here, we con-
 96 sider polymers with N Kuhn segments of which $Z_s \ll N$
 97 are chemically identical stickers. The non-sticky seg-
 98 ments are always open, while the stickers may switch be-
 99 tween open and closed states with rates k_{close} and k_{open} .
 100 The opening rate is approximately constant if the force
 101 within the chain does not significantly decrease the ac-
 102 tivation energy for sticker dissociation. For instance, for
 103 silk the activation barrier is $8k_B T \approx 24 \text{ pN} \cdot \text{nm}$ [14] and
 104 instantaneous bond dissociation over 0.1 nm requires ap-
 105 proximately a force of 240 pN. **To produce this force, f ,**
 106 **chain alignment alone is not enough ($3k_B T/a$)** while by
 107 Gaussian stretching [46]

$$f = 3k_B T (R_s - R_{s,0}) / R_{s,0}^2, \quad (4)$$

108 it would be required to stretch the quiescent distance be-
 109 tween stickers, $R_{s,0} \approx 9 \text{ nm}$, [47] to $R_s \approx 1800 \text{ nm}$ (**using**
 110 **the sticker- rather than the entanglement strand tacitly**
 111 **assumes $Z_s \gtrsim Z_e$). On the other hand, full extension**
 112 **of the substrand between stickers is already achieved at**
 113 $R_s \approx 200 \text{ nm}$ [48]: in practice, therefore it seems likely
 114 the destabilization of the stickers by the chain tension oc-
 115 curs, for silk, in the same regime where finite-extensibility
 116 effects emerge [49]. By approximating k_{open} as a con-
 117 stant, it can be related to the rheological sticker lifetime
 118 as $\tau_s = k_{\text{open}}^{-1}$ [14, 19, 26, 28–31], and the closing rate
 119 is given by $k_{\text{close}} = k_{\text{open}} p / (1 - p)$, with p the time- or
 120 ensemble-averaged fraction of closed stickers. Hence, we
 121 will treat p and τ_s as free model parameters [19].

122 We have benchmarked our model in the absence of
 123 flow using the Likhtman-McLeish model for linear non-
 124 sticky polymers [35] (this linear rheological response is
 125 not shown here) and using the sticky-Rouse diffusivity,
 126 $D_{\text{SR}} = D_{\text{SR}}(Z_e, \tau_e, Z_s, \tau_s, p)$ as calculated by Leibler et

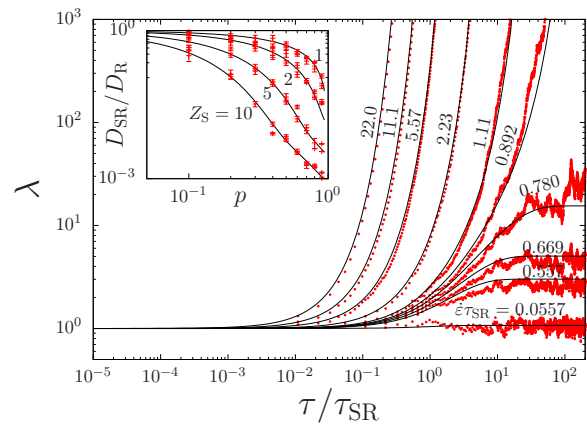


FIG. 1. Comparison between the stretch ratio λ of a sticky polymer ($Z_e = Z_s = 10$, $\tau_s = 10^4 \tau_e$, $p = 0.95$, $Z_s = 10$) against time t in units of the sticky Rouse time τ_{SR} at a range of flow rates from $\dot{\epsilon} = 0.056\tau_{\text{SR}}^{-1}$ to $22.3\tau_{\text{SR}}^{-1}$ in logarithmic steps. The sticky Rouse time is $\tau_{\text{SR}} = [D_{\text{R}}/D_{\text{SR}}]\tau_{\text{R}}$ with D_{R} the bare Rouse diffusivity, $\tau_{\text{R}} = \tau_e Z_e^2$ the bare Rouse time and D_{SR} the sticky diffusivity (see inset). In the main panel, the symbols are obtained by averaging over five Brownian dynamics simulations with different random number seeds; the lines represent the single-mode model in Eq. (5). The inset shows consistence of the simulated sticky-Rouse diffusivity (symbols; averaged over 25 random number seeds) with the sticky-reptation model (lines) of Leibler *et al.* [19].

127 al. [19] (see the inset of Figure 1). For the non-linear
 128 dynamics of sticky polymers, so far no comparisons be-
 129 tween analytical predictions with simulations or experi-
 130 ments have been reported. The first strategy to address
 131 this is to evaluate how well a DEMG-type single-mode
 132 approximation performs [49], with chain friction renor-
 133 malized by averaging over the stochastic sticker dynam-
 134 ics:

$$\frac{d\lambda}{dt} = \dot{\epsilon}\lambda + \frac{1}{\tau_{\text{SR}}}(1 - \lambda) \quad (5)$$

135 where the stretch ratio, $\lambda \equiv (R_N - R_1)/Z_e$, is presumed
 136 to be uniform over the backbone of the chain. The exten-
 137 sion rate is proportional to the stretch ratio itself. The
 138 retraction rate is determined by $(1 - \lambda)$ (in the absence
 139 of flow, $\lambda = 1$ at steady state) and by the sticky-Rouse
 140 time, $\tau_{\text{SR}} \equiv [D_{\text{R}}/D_{\text{SR}}]\tau_s$. In the main graph of Figure 1,
 141 we present comparison between this simple approxima-
 142 tion and our simulations, (the approximations inherent
 143 in the DEMG require that the simulation time be divided
 144 by a factor 1.2 to result in the close agreement shown).
 145 This confirms that the intuitive ‘sticky Weissenberg num-
 146 ber’ for the stretch transition is $\text{Wi} = \dot{\epsilon}\tau_{\text{SR}}$. For $\text{Wi} > 1$
 147 an exponential runaway stretch emerges as expected. In
 148 contrast to non-sticky polymers, however, we will argue
 149 that the stress and fluctuation in stretch may diverge
 150 below this stretch transition when the pre-averaging ap-
 151 proximation inherent in DEMG is avoided.

152 While non-sticky polymers in steady state show a
 153 Gaussian stretch distribution with a width that is de-
 154 termined by the (effective) number of entanglements, we
 155 have observed rather large stretch fluctuations for the
 156 sticky polymer at extension rates of the order of, but be-
 157 low, the critical value. Indeed, the symbols in Figure 1
 158 are averaged over five simulations for a chain with 10
 159 stickers which are on average closed a fraction $p = 0.95$
 160 of time. For simulations with $p < 0.9$ these fluctuations
 161 become much larger and difficult to distinguish graphi-
 162 cally. Indeed, while the mean stretch is finite, the fluctu-
 163 ations in stretch diverge above a certain flow rate *below*
 164 the stretch transition.

165 For three of the flow rates shown in Figure 1 we have
 166 plotted the stretch distribution, $P(\lambda)$, in Figure 2. For
 167 small flow rates, the stretch distribution is Gaussian,
 168 $\ln P(\lambda) \propto (1-\lambda)^2$ (solid curves), as in the quiescent state.
 169 However, for increased flow rates deviations emerge in the
 170 high- λ tail of the distribution. Importantly, the polymer
 171 stretch may resemble the mean stretch for long times
 172 compared to the sticky-Rouse time, and only in ‘rare
 173 events’ the stickers may remain closed sufficiently long
 174 for the stretch to reach deep into the tail of the distribu-
 175 tion (see inset).

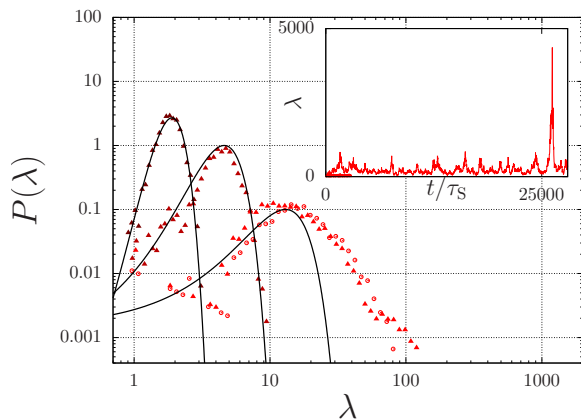


FIG. 2. The steady-state probability distribution, $P(\lambda)$, is plotted against the stretch ratio, λ . The symbols are obtained from the steady-state simulations of Fig. 1 at the flow rates ($\dot{\epsilon}\tau_{\text{SR}} = 0.446, 0.668$ and 0.780 ; the curves are Gaussian fits. For an increasing flow rate, the high-stretch tail is no longer Gaussian but becomes a power law, $P(\lambda) \propto \lambda^{-\nu}$. The inset shows the stretch ratio against time for $\dot{\epsilon}\tau_{\text{SR}} = 0.780$ and visualizes how this distribution includes ‘rare events’ of enormous chain stretch. For a sufficiently large flow rate, ν decreases. If $\nu > 2$, the mean value of λ is finite (as it should in steady state); however, if also $\nu \leq 3$, the fluctuations in stretch, characterized by the expectation value of λ^2 , diverge.

In the following, we will explore the problem analytically using a ‘sticky dumbbell model’ to explore and clarify the underlying causes of the power-law tail in the stretch distribution, and explore how it can be tuned by the flow rate. This minimal model that captures the

essential physics is equivalent to a single polymer strand either attached to the bulk deformation at both ends (the closed state) or free to relax (the open state). The rate by which the polymer switches between the two states is given by the usual opening and closing rates. We can now address the development of stretch under extensional flow through a pair of coupled partial differential equations for the time-dependent stretch distributions $P_o(t, \lambda)$ and $P_c(t, \lambda)$ for each state using the master equation

$$\begin{aligned} \frac{\partial P_c}{\partial t} &= -\frac{\partial}{\partial \lambda} [P_c \dot{\epsilon} \lambda] - k_{\text{open}} P_c - k_{\text{close}} P_o, \\ \frac{\partial P_o}{\partial t} &= -\frac{\partial}{\partial \lambda} \left[P_o \left(\dot{\epsilon} \lambda + \frac{1-\lambda}{\tau_R} \right) \right] + k_{\text{open}} P_c - k_{\text{close}} P_o. \end{aligned} \quad (6)$$

176 Note that this evolution equation invokes a single-mode
 177 approximation and ignores thermal fluctuations: the
 178 stretch distribution emerges from the coupling between
 179 a closed state in which the polymer is stretched and the
 180 open state in which it can retract. Under strong flow
 181 conditions, the effective driving noise is completely domi-
 182 nated by the stochastic state-switching, with thermal
 183 noise negligible.

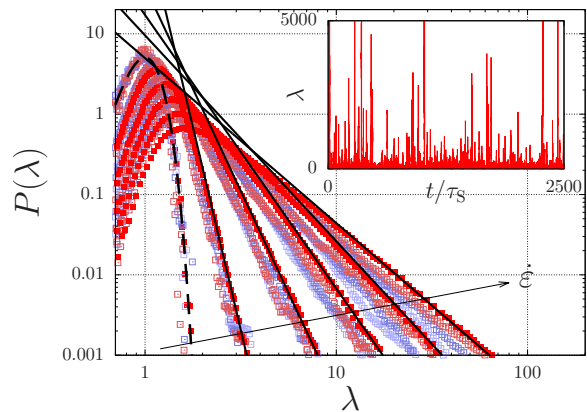


FIG. 3. The power-law stretch distribution, $P(\lambda) \propto \lambda^{-\nu}$ for large λ , observed in Fig. 2 is replicated analytically in a sticky dumbbell model for a sticky polymer ($Z_e = 10$, $p = 0.9$, $\tau_s = 1000\tau_e$), which has two stickers near the end of the chain that are simultaneously either open or closed (lines). The dashed curve is the Gaussian stretch distribution under quiescent conditions. In linear steps, the flow rate is increased up to $\dot{\epsilon}\tau_R = 0.05$. The symbols are obtained in simulations with 2, 6, 12 and 36 beads (from red to light blue). For small flow rates, where $\nu < 3$, the simulated power-law tails of $P(\lambda)$ (symbols) are in agreement with Eq. (8). The inset shows the transient behavior of the simulation with $\dot{\epsilon}\tau_R = 0.05$.

184 We calculate the steady-state stretch distribution at
 185 strong stretch by setting the left-hand side of Eq. (6) to
 186 zero and taking $\lambda \gg 1$. The result can be solved ana-
 187 lytically since in these conditions the differential system
 188 becomes homogeneous. We therefore find the power-law

189 relation

$$P(\lambda) \propto \lambda^{-\nu}, \quad (7)$$

190 with the exponent given in terms of the three dimension-
191 less parameters of the system, p , $\dot{\epsilon}\tau_R$, τ_R/τ_s by

$$\nu = 1 + \frac{1}{1 - \dot{\epsilon}\tau_R} \frac{p}{1 - p} \frac{\tau_R}{\tau_s} - \frac{1}{\dot{\epsilon}\tau_s}. \quad (8)$$

192 We compare this power-law to our sticky dumbbell simu-
193 lations in Figure 3. In passing, we note that this model
194 also provides an example of one of a family of driven,
195 stochastic, systems together referred to as ‘multifractals’
196 [50] in which a divergent and scaling structure of fluctua-
197 tions arises, not just at a single critical point, but within
198 a large region of state space, and with a universal critical
199 exponent replaced by a family, dependent on the degree of
200 forcing.

201 For sufficiently small flow rates, we find a reasonable
202 agreement between our multibead simulations and the
203 analytical approximation for the simple sticky dumbbell
204 (under these conditions, $\nu > 3$). While the simula-
205 tion for chains with just two beads (i.e., with a single
206 Rouse mode) agrees well with the approximate theory,
207 the higher Rouse modes in the multibead chain provide
208 an additional relaxation mechanism for the retraction of
209 the chain ends alike contour-length fluctuations. Hence,
210 the single-mode approximation slightly overestimates the
211 width of the stretch distribution of a real chain (i.e., a
212 multibead chain). The discrepancy between the single-
213 mode and multibead chain becomes apparent if the flow
214 rates are high for the exponent ν to approach or go be-
215 yond a value 3 (this occurs at $(1 - p)\dot{\epsilon}\tau_R \approx \tau_R/(2\tau_s)$).
216 This is not a coincidence: if $\nu = 3$ the magnitude of the
217 fluctuations diverge, $\langle \lambda^2 \rangle \rightarrow \infty$. Although the fluctua-
218 tions diverge for $\nu = 3$, the mean $\langle \lambda \rangle$ remains finite as
219 long as $\nu \leq 2$ (the equality holds approximately when
220 $(1 - p)\dot{\epsilon}\tau_R \approx \tau_R/\tau_s$). For even larger flow rates, i.e., for
221 $\nu \leq 1$ (at $(1 - p)\dot{\epsilon}\tau_s = 1$) the stretch distribution can no
222 longer be normalized and true runaway stretch emerges.
223 These various regimes are displayed in Figure 4 in terms
224 of the dimensionless parameters of the system. Note that
225 the stress is $\sigma \propto (1 - \lambda)^2$ and the tail of the stress dis-
226 tribution is $P(\sigma) \propto \lambda^{-\nu/2}$: the mean stress diverges for
227 $\nu \leq 4$ and its variance diverges for $\nu \leq 6$.

228 The single-mode dumbbell model clarifies the route
229 through which the divergent fluctuations arise. Crucially,
230 when a stretched strand is freed from the network, it may
231 not relax entirely before reattachment (this effect is ig-
232 nored in classical treatments of transient network models,
233 which in consequence overlook the strong stochastic fluctua-
234 tions they physically imply). Such continuous inter-
235 change between convecting and relaxing strands, together
236 with the occurrence of longer-than-average attachment
237 times for some segments, allow the exploration of very
238 large chain stretches in steady-state.

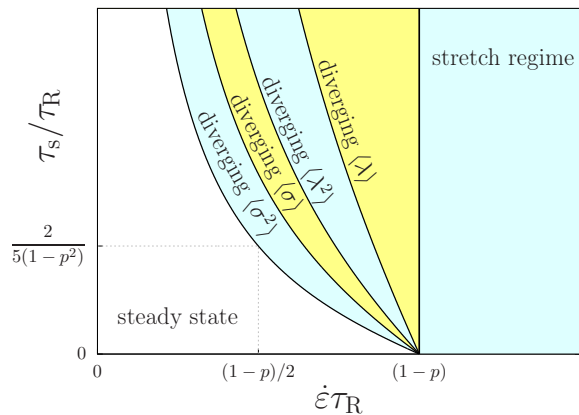


FIG. 4. State diagram of a sticky dumbbell. For a short sticker lifetime, polymer stretching takes place if the Weissenberg number, $(1 - p)\dot{\epsilon}\tau_R$, is larger than unity. p is the time-averaged fraction of closed stickers and τ_R is the bare Rouse time. For a finite sticker lifetime, the mean and the variance of the stress, σ , and the stretch, λ , diverge in different regimes. The curves are given by Eq. 8 for $\nu = 2, 3, 4, 6$ as discussed in the main text.

239 To illustrate the potential consequences of this effect,
240 we consider nucleation rates in steady-state extensional
241 flow, assuming that polymer crystal phase may nucleate
242 around chains beyond a critical stretch ratio λ_* [1]. As-
243 suming that the chain is relaxed prior to sticker closing at
244 time $t = 0$, its stretch ratio develops as $\lambda(t) = \exp(\dot{\epsilon}t)$ un-
245 til it opens at a time τ_{open} . This time is drawn from the
246 probability distribution $p(\tau_{\text{open}}) = \tau_s^{-1} \exp(-\tau_{\text{open}}/\tau_s)$,
247 so the probability that the critical stretch is reached is
248 $p_* = \lambda_*^{-1/\dot{\epsilon}\tau_s}$. The probability that λ_* is not reached af-
249 ter n attempts is $(1 - p_*)^n$, and therefore the expected
250 number of attempts needed is

$$\langle n \rangle = \frac{\sum_{n=1}^{\infty} n(1 - p_*)^n}{\sum_{n=1}^{\infty} (1 - p_*)^n} = \lambda_*^{1/(\dot{\epsilon}\tau_s)}. \quad (9)$$

251 An attempt occurs, on average, after time intervals
252 $1/k_{\text{open}} + 1/k_{\text{close}} = \tau_s/p$. If the number density
253 of chains is ρ , then combining these results gives an
254 extension-rate-dependent nucleation rate per volume $J =$
255 $[\rho p/\tau_s] \lambda_*^{-1/(\dot{\epsilon}\tau_s)}$. We expect that the form

$$\ln J = A - \frac{B}{\dot{\epsilon}\tau_s}, \quad (10)$$

256 with A and B flow-independent coefficients, carries over
257 to the multi-sticker chain provided that the substrand
258 between stickers is sufficiently long and τ_s can be treated
259 as a constant (see our discussion on Eq. (4)). This consti-
260 tutes a first prediction for the rate of flow-induced crys-
261 tallization of associating polymers in steady-state exten-
262 sional flow, which along with the prediction of strong
263 stretch fluctuations will help the interpretation of the
264 (noisy) non-linear rheology of silk [9, 16], e.g., using con-
265 focal microscopy [51] and controlled variations of ionic

content in the solution [52], and thereby aid the development of its synthetic counterparts [15].

In conclusion, we have numerically solved the 1D stochastic Langevin equation of an aligned entangled sticky polymer in an effective medium and in extensional flow. We show that this computationally inexpensive simulation method captures the combined polymer physics of reptation, contour-length-fluctuations and response in extensional flow, associating stickers. Crucially, it does not pre-average any fluctuations in chain stretch, and predicts that in steady-state flow a small number of chains (rather than all of them) stretches to a large extent: this seems a promising energy-efficient strategy to trigger the flow-induced crystallisation of polymers. **For quantitatively accurate simulations, it will be essential to include a description for finite chain extensibility, as well as a description for the chain stretch reducing the sticker binding energy and hence their lifetime.**

This research was funded by the Engineering and Physical Sciences Research Council [grant number EPSRC (EP/N031431/1)]. Jorge Ramírez is thanked for sharing Alexei Likhtman's Brownian dynamics code and Richard Graham is thanked for sharing his GLaMM code; both codes helped us to benchmark our simulation software. Chris Holland and Pete Laity are thanked for useful and encouraging discussions.

* charley.schaefer@york.ac.uk

- [1] R. S. Graham and P. D. Olmsted, *Phys. Rev. Lett.* **103**, 115702 (2009).
- [2] E. M. Troise, H. J. M. Caelers, and G. W. M. Peters, *Macromolecules* **50**, 3868 (2017).
- [3] D. A. Nicholson and G. C. Rutledge, *J. Rheol.* **63**, 465 (2019).
- [4] S. Moghadamand, I. S. Dalal, and R. G. Larson, *Macromolecules* **52**, 1296 (2019).
- [5] D. J. Read, C. McIlroy, C. Das, O. G. Harlen, and R. S. Graham, *Phys. Rev. Lett.* **124**, 147802 (2020).
- [6] T. Asakura, H. Suzuki, and Y. Watanabe, *Macromolecules* **16**, 1024 (1983).
- [7] T. Asakura, Y. Watanabe, A. Uchida, and H. Minagawa, *Macromolecules* **17**, 1075 (1984).
- [8] C. Zhao and T. Asakura, *Prog. Nucl. Magn. Reson. Spectrosc.* **39**, 301 (2001).
- [9] N. Kojić, J. Bico, C. Clasen, and G. H. McKinley, *J. Exp. Bio.* **209**, 4355 (2006).
- [10] C. Holland, F. Vollrath, A. J. Ryan, and O. O. Mykhaylyk, *Adv. Mater.* **24**, 105 (2012).
- [11] T. Asakura, K. Okushita, and M. P. Williamson, *Macromolecules* **48**, 2345 (2015).
- [12] P. R. Laity, S. E. Gilks, and C. Holland, *Polymer* **67**, 28 (2015).
- [13] P. R. Laity and C. Holland, *Biomacromolecules* **17**, 2662 (2016).
- [14] C. Schaefer, P. R. Laity, C. Holland, and T. C. B. McLeish, *Macromolecules* **53**, 2669 (2020).
- [15] G. J. Dunderdale, S. J. Davidson, A. J. Ryan, and O. O. Mykhaylyk, *Nat. Comm.* **11**, 3372 (2020).
- [16] A. Koepfel, P. R. Laity, and C. Holland, *Soft Matter* **14**, 8838 (2018).
- [17] P. R. Laity, E. Baldwin, and C. Holland, *Macromol. Biosci.* **0**, 1800188 (2018).
- [18] O. Kramer, *Biological and synthetic polymer networks* (Elsevier Applied Science, New York, NY, 1988).
- [19] L. Leibler, M. Rubinstein, and R. H. Colby, *Macromolecules* **24**, 4701 (1991).
- [20] R. A. Weiss, J. J. Fitzgerald, and D. Kim, *Macromolecules* **24**, 1071 (1991).
- [21] T. Annable, R. Buscall, R. Ettelaie, and D. Whittlestone, *J. Rheol.* **37**, 695 (1993).
- [22] R. H. Colby, X. Zheng, M. H. Rafailovich, J. Sokolov, D. G. Peiffer, S. A. Schwarz, Y. Strzhemechny, and D. Nguyen, *Phys. Rev. Lett.* **81**, 3876 (1998).
- [23] R. A. Weiss and W. C. Yu, *Macromolecules* **40**, 3640 (2007).
- [24] S. Seiffert and J. Sprakel, *Chem. Soc. Rev.* **41**, 909 (2012).
- [25] S. Hackelbusch, T. Rossow, P. van Assenbergh, and S. Seiffert, *Macromolecules* **46**, 6273 (2013).
- [26] Z. Zhang, Q. Chen, and R. H. Colby, *Soft Matter* **14**, 2961 (2018).
- [27] T. Yamane, K. Umemura, Y. Nakazawa, and T. Asakura, *Macromolecules* **36**, 6766 (2003).
- [28] Q. Chen, Z. Zhang, and R. H. Colby, *J. Rheol.* **60**, 1031 (2016).
- [29] T. Tomkovic and S. G. Hatzikiriakos, *J. Rheol.* **62**, 1319 (2018).
- [30] T. Tomkovic, E. Mitsoulis, and S. G. Hatzikiriakos, *Phys. Fluids* **31**, 033102 (2019).
- [31] M. Zuliki, S. Zhang, K. Nyamajaro, T. Tomkovic, and S. G. Hatzikiriakos, *Phys. Fluids* **32**, 023104 (2020).
- [32] G. Cui, V. A. H. Boudara, Q. Huang, G. P. Baeza, A. J. Wilson, O. Hassager, D. J. Read, and J. Mattsson, *J. Rheol.* **62**, 1155 (2018).
- [33] P. G. de Gennes, *J. Chem. Phys.* **55**, 572 (1971).
- [34] M. Doi and S. F. Edwards, *The Theory of Polymer Dynamics* (Clarendon, Oxford, 1986).
- [35] A. E. Likhtman and T. C. B. McLeish, *Macromolecules* **35**, 6332 (2002).
- [36] A. E. Likhtman and R. S. Graham, *J. Non-Newtonian Fluid Mech.* **114**, 1 (2003).
- [37] V. A. H. Boudara and D. J. Read, *J. Rheol.* **61**, 339 (2017).
- [38] V. A. H. Boudara, D. J. Read, and J. Ramírez, *J. Rheol.* **64**, 709 (2020).
- [39] M. W. Collis, A. K. Lele, M. R. Mackley, R. S. Graham, D. J. Groves, A. E. Likhtman, T. M. Nicholsona, O. G. Harlen, T. C. B. McLeish, L. R. Hutchings, C. M. Fernyhough, and R. N. Young, *J. Rheol.* **49**, 501 (2005).
- [40] M. Doi, *J. Polym. Phys.* **21**, 667 (1983).
- [41] R. S. Graham, A. E. Likhtman, T. C. B. McLeish, and S. T. Milner, *J. Rheol.* **47**, 1171 (2003).
- [42] D. Auhl, P. Chambon, T. C. B. McLeish, and D. J. Read, *Phys. Rev. Lett.* **103**, 136001 (2009).
- [43] M. S. Green and A. V. Tobolsky, *J. Chem. Phys.* **14**, 80 (1946).
- [44] F. Smallenburg, L. Leibler, and F. Sciortino, *Phys. Rev. Lett.* **111**, 188002 (2013).
- [45] S. Ciarella, F. Sciortino, and W. G. Ellenbroek, *Phys. Rev. Lett.* **121**, 058003 (2018).
- [46] M. Rubinstein and R. H. Colby, *Polymer Physics*, 4th ed.

- (Oxford University Press, Oxford, 2003).
- [47] From the end-to-end distance $R_e = Z_s^{1/2} R_s$ with $Z_s = 5 - 10$ [14] and $R_e = \sqrt{6} R_g$ with $R_g = 10$ nm [13], we have $R_{s,0} = 7.9 - 11$ nm.
- [48] The step size of an amino acid is 0.36 nm and silk has substrands of 550 amino acids between stickers [13, 14].
- [49] J. M. Dealy, D. J. Read, and R. G. Larson, *Structure and Rheology of Molten Polymers* (Hanser, Munich, 2018).
- [50] D. Harte, *Multifractals* (Chapman and Hall/CRC, New York, 2001).
- [51] C. Holland, J. Urbach, and D. L. Blair, *Soft Matter* **8**, 2590 (2012).
- [52] A. Koepfel, P. R. Laity, and C. Holland, *Acta Biomaterialia* **117**, 204 (2020).